A&A 580, L10 (2015)
DOI: 10.1051/0004-6361/201526377

Astronomy & Astrophysics

Letter to the Editor

First detection of the 63 μm atomic oxygen line in the thermosphere of Mars with GREAT/SOFIA⋆

L. Rezac[1], P. Hartogh[1], R. Güsten[2], H. Wiesemeyer[2], H.-W. Hübers[3,4], C. Jarchow[1], H. Richter[3], B. Klein[2,6], and N. Honingh[5]

[1] Max-Planck-Institut für Sonnensystemforschung, Justus-von-Liebig-Weg 3, 37077 Göttingen, Germany
e-mail: rezac@mps.mpg.de
[2] Max-Planck-Institut für Radioastronomie, Auf dem Hügel 69, 53121 Bonn, Germany
[3] Deutsches Zentrum für Luft- und Raumfahrt e.V., Institute of Optical Sensor Systems, Rutherfordstr. 2, 12489 Berlin, Germany
[4] Humboldt-Universität zu Berlin, Department of Physics, Newtonstr. 15, 12489 Berlin, Germany
[5] Physikalisches Institute der Universität zu Köln, Zülpicher Str. 77, 50937 Köln, Germany
[6] University of Applied Sciences Bonn-Rhein-Sieg, Grantham-Allee 20, 53757, Sankt Augustin, Germany

Received 21 April 2015 / Accepted 27 July 2015

ABSTRACT

Context. The Stratospheric Observatory for Infrared Astronomy (SOFIA) with its 2.5 m telescope provides new science opportunities for spectroscopic observations of planetary atmospheres in the far-infrared wavelength range.
Aims. This paper presents first results from the 14 May, 2014 observing campaign of the Martian atmosphere at 4.7 THz using the German REceiver for Astronomy at Terahertz frequencies (GREAT) instrument.
Methods. The atomic oxygen 63 μm transition, OI, was detected in absorption against the Mars continuum, with a high signal-to-noise ratio (~35). A beam-averaged atomic oxygen from a global circulation model was used as input to the radiative transfer simulations of the observed line area and to obtain a new estimate on the column density using a grid-search method.
Results. Minimizing differences between the calculated and observed line intensities in the least-square sense yields an atomic oxygen column density of $(1.1 \pm 0.2) \times 10^{17}$ cm^{-2}. This value is about twice as low as predicted by a modern photochemical model of Mars. The radiative transfer simulations indicate that the line forms in the upper atmospheric region over a rather extended altitude region of 70–120 km.
Conclusions. For the first time, a far-infrared transition of the atomic oxygen line was detected in the atmosphere of Mars. The absorption depth provides an estimate on the column density, and this measurement provides additional means to constrain the photochemical models in global circulation models and airglow studies. The lack of other means for monitoring the atomic oxygen in the Martian upper atmosphere makes future observations with the SOFIA observatory highly desirable.

Key words. planets and satellites: atmospheres – planets and satellites: individual: Mars – planets and satellites: detection – line: profiles

1. Introduction

Atomic oxygen is the key element in several processes governing the energy and mass flow in the mesosphere-thermosphere-ionosphere of Mars. It controls the radiative cooling from the CO_2 15 μm bands in the Martian thermosphere (Bougher & Roble 1991). Atomic oxygen also plays a significant role in establishing the local exobase height (varying from 155–190 km between night and day), thereby affecting the ion production, plasma heating, and ultimately the atmospheric erosion through escape processes (Leblanc & Johnson 2002; Valeille et al. 2010).

Despite the recognized need for accurate knowledge of atomic O abundances in the upper atmosphere, there have been only a few dedicated measurements. The analysis of UV airglow measurements at 130.4 nm from the Mariner 6, 7, and 9 flybys (1969, 1971) provided the first information on the relative abundance of atomic O (Barth et al. 1972). Stewart et al. (1992) reanalyzed the Mariner 9 measurements and compared the results with a thermospheric general circulation model to explain the considerable local time variation in atomic O. These measurements were consistent with afternoon atomic O density being higher than in the morning observations, a behavior not yet reproduced by the models (Valeille et al. 2010). Since atomic O has a multitude of electronic transitions, different spectral regions may be used in estimating the O abundances, for example, 557 and 663 nm (Krasnopolsky & Krysko 1976; Krasnopolsky & Feldman 2002). Oxygen abundances were also estimated from the CO_2^+ number density (Stewart et al. 1992) and from ion data (Hanson et al. 1977). The more recent Mars Express mission (2003) carries a UV spectrometer (SPICAM) that also measures the O(130.4 nm) electronic transition (Bertaux et al. 2006), but to our knowledge, the O density has not yet been derived below the exobase (Chaufray et al. 2009). A powerful imaging spectrograph (UVIS) onboard the MAVEN spacecraft, which arrived at Mars in September 2014, also aims at obtaining the atomic O density from the UV airglow at 130.4 nm (McClintock et al. 2014). The mass spectrometer NGIMS on the same satellite may obtain O density (Mahaffy et al. 2014) down to ≈150 km. While sensing the UV emissions from neutral and/or ionic species is very suitable for probing the upper atmosphere state, extracting

⋆ Appendix A is available in electronic form at http://www.aanda.org

the reliable information on the neutral atmosphere (especially the atomic oxygen) is a challenging task. Complex modeling is needed because of the various energy sources and chemical pathways that generate and/or contaminate (scattering, dust opacity) the observed UV emissions (Chaufray et al. 2009; Huestis et al. 2010). To date, the only in situ (although not direct) determination of the atomic O density has been made from the data of the neutral mass spectrometer taken during the descent of the Viking 1 and 2 landers in the Martian atmosphere. These data revealed that CO_2 is the main component of the Martian atmosphere below ~180 km (with the homopause at ~125 km) and that atomic O is the most abundant among the odd-oxygen compounds (McElroy et al. 1976; Nier & McElroy 1977).

The electronic ground state of atomic oxygen, $O(^3P)$, is a triplet state with transition frequencies falling into the far-infrared spectrum. The 63 μm, ($^3P_1$–$^3P_2$), transition has been observed in astrophysical contexts, such as molecular clouds and star-forming regions. However, this is only possible from satellite platforms, aircraft, or balloon-mounted instruments since the water vapor opacity in the Earth's troposphere is completely opaque to the far-IR photons. This transition has also been periodically observed in Earth's thermosphere (Mlynczak et al. 2004). In this paper we report for the first time on the observation of this transition in another planet and on the potential for systematically monitoring the thermospheric atomic O on Mars using the modern SOFIA/GREAT instrument.

The paper is structured as follows: Sect. 2 provides the description of the instrumental setup, details on the observation, and data calibration. Then an analysis of the observation is presented to derive the atomic O column density. In the last section we summarize the science results and implication for future observations.

2. Observations

While far-infrared observations of O_2 in the Martian atmosphere were performed for the first time (Hartogh et al. 2010a) with *Herschel*/HIFI (de Graauw et al. 2010) as part of the HssO key program (Hartogh et al. 2009), the atomic oxygen line at 63 μm, [OI], observed in absorption against the continuum of Mars, was for the first time detected using the GREAT[1] instrument (Heyminck et al. 2012) onboard the SOFIA aircraft. The observations were performed on a high-altitude flight (13 km) out of Palmdale, California, on May 14, 2014 during good observing conditions (PWV 11 μm, and T_{sys} = 3684 K). The observing conditions for the planet are summarized in Table 1.

The high-resolution spectrometer GREAT for the first time operated its H-channel, tuned to the ground-state transition of [OI] at 4744.77749 GHz. Major technological breakthroughs enabled these observations: a superconducting NbN hot-electron bolometer (HEB) waveguide mixer (Büchel et al. 2015), pumped by a novel quantum-cascade laser (QCL; Richter et al. 2015) as local oscillator provides receiver temperatures as low as 1000 K. The data were processed in a new-generation fast Fourier transform spectrometer (Klein et al. 2012), providing a 44 kHz spectral resolution over a 2.5 GHz bandwidth.

During this first technology demonstration, the QCL was not frequency locked, drifting by several 10 MHz with time and revealing an "intrinsic" width of about 10 MHz (on the timescale of our data dump cycle of 0.5 to 1 s). We took advantage of the prominent, narrow terrestrial OI line measured simultaneously in our spectrum (only shifted 132 MHz from the martian OI line) to correct for these frequency drifts (see next section).

The boresight and focus position of the GREAT instrument was determined on Mars just before the OI spectroscopy. The source coupling efficiency (η_s = 0.67) and beamwidth (6.6″) of the H-channel were derived from scans across the planet. The SOFIA optical guide cameras established pointing to an accuracy of a few arcsecs. The OI spectroscopy was performed in double-beam chopped mode for a total of 45 min, with a chop rate of 1 Hz and a throw of ±40″. The Doppler correction changed by only +0.005 km s^{-1} within the integration time.

The measured spectra are shown in Fig. 1 panel A, covering both transitions. In panel B a zoom-in of the Martian spectrum is shown, with an apparent linewidth of 26 MHz (symetrized FWHM). Both lines are broader than expected from pure Doppler broadening (11 MHz FWHM at 180 K), which is the dominant broadening mechanism of this transition in both

Table 1. Mean observing conditions of Mars, May 14, 2014.

Condition	Value
Heliocentric distance	1.59 AU
Geocentric distance	0.70 AU
Apparent diameter	13.45″
Geocentric velocity	8.31 km s^{-1}
Phase angle	26°
Ls	130°
ΔRA beam	1.2″
ΔDec beam	0.2″
Mean T_{surf}	(269 ± 15) K
Mean p_{surf}	(6.64 ± 0.84) mbar

Notes. Mean surface pressure and temperature are from the v5.2 Mars climate database averaged over the field of view (http://www-mars.lmd.jussieu.fr). Standard deviation is provided to indicate the modeled variability within the sampled beam. Geocentric velocity from SOFIA's observing coordinates (42N, 123W). The continuum emissions at 63 μm are understood to originate up to several wavelengths below the surface, therefore, the brightness temperatures are expected to be lower than the surface temperatures). The ΔRA and ΔDec represent the beam center pointing offset with respect to the disk center.

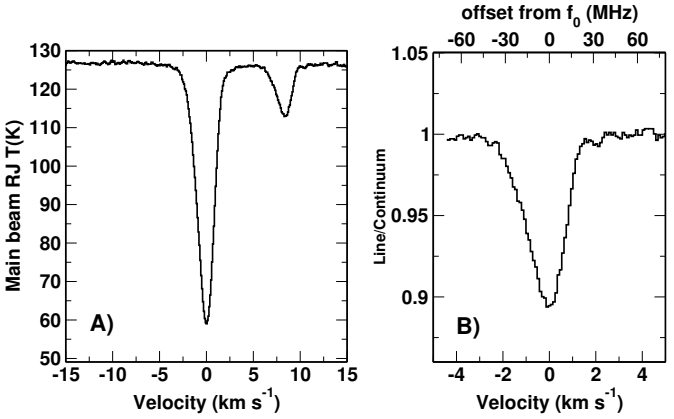

Fig. 1. Panel **A)**: measured spectra centered at the telluric line demonstrating a clear detection of the atomic O in both atmospheres. The scale is in Raleigh-Jeans main beam temperature [K], single side-band calibration. Panel **B)**: only the Martian line already corrected for Doppler velocity and plotted as line/continuum ratio. A third-degree baseline correction was applied to this spectrum.

[1] GREAT was developed by the MPI für Radioastronomie and the KOSMA/Universität zu Köln, in cooperation with the MPI für Sonnensystemforschung and the DLR Institut für Planetenforschung.

atmospheres. This most likely reflects the intrinsic line width (10–20 MHz) of the reference signal from the QCL that during this experiment was not frequency stabilized to the required precision. Slow frequency drifts were corrected against the frequency of the telluric OI line seen in the normalized sky spectrum, but jitter on timescales shorter than our integration time of 0.5–1 s per phase remained. The convolution of this intrinsic OI and instrumental QCL line shapes was incorporated into our modeling and is described below.

3. Data analysis

The residual Doppler shift of the measured lined was detected, but we were unable to obtain a reliable estimate on the mean winds due to the uncertainty in the estimated accuracy of the frequency scale (±90 m/s). We also studied the asymmetric blue wing of the line, (see Fig. 1), with synthetic forward calculations using realistic wind vertical profiles (which can peak in the range 100–250 m/s at 90–120 km) on Mars as provided by the Laboratoire de Météorologie Dynamique (LMD) Mars General Circulation Model data, (Forget et al. 1999), available through the v5.2 Mars Climate Database (MCD). It was found that an asymmetric line profile can develop for an optical depth >1. However, this happens only if the maximum wind speed is present on the line of sight. This situation is unlikely to occur, given the nearly disk-centered beam of our observing geometry, including the 2″ uncertainty in the absolute pointing. Additionally, we were unable to easily explain the overall redshift of the line with the strong blue-wing asymmetry in our modeling. Therefore, we consider the possibility that the asymmetric line shape is at least partially due to yet unknown instrumental effects (most likely a feature of the QCL), and the further analysis relies on the symmetrized lines shape.

Modeling input parameters of the Martian atmosphere were taken from the v5.2 MCD, and the beam averaged temperature, pressure and atomic O volume mixing ratio (VMR) profiles for a given observing geometry, season, and local time were calculated (see Fig. A.1). A forward line-by-line (LBL) radiative transfer model described in Jarchow & Hartogh (1995) that was previously applied to Mars (Hartogh et al. 2010b) and Venus (Rengel et al. 2008) was used to calculate beam-averaged synthetic spectra in spherical geometry. The broadening due to planet rotation is negligible for this transition given the subobserver latitude, rotational axis tilt, and beam center offset (1″ from the central meridian), even though it was taken into account in our simulations. The line shape was modeled with a Voigt profile. The line center rest frequency was measured by Zink & Evenson (1991), and other spectroscopic line parameters were taken from HITRAN 2012 (Rothman et al. 2013). The default (no-knowledge) value for the half-width of the Lorenzian component,(0.05 cm^{-1}/atm) was provided by the HITRAN database. Because there is no estimate on the actual value of the collisional broadening, we performed a sensitivity test by increasing the coefficient ten times. Even at this value, the collisional broadening is negligible, and the Doppler broadening regime dominates above ≈5 km. The electronic partition function and stimulated emission term for scaling line intensity to atmospheric temperature is significantly different from unity and was explicitly calculated using fine-structure level energies and prescribed degeneracies from HITRAN 2012. Over the range of pressures where the line forms, we can assume that the local thermodynamic equilibrium (LTE) applies for the transition (Sharma et al. 1994).

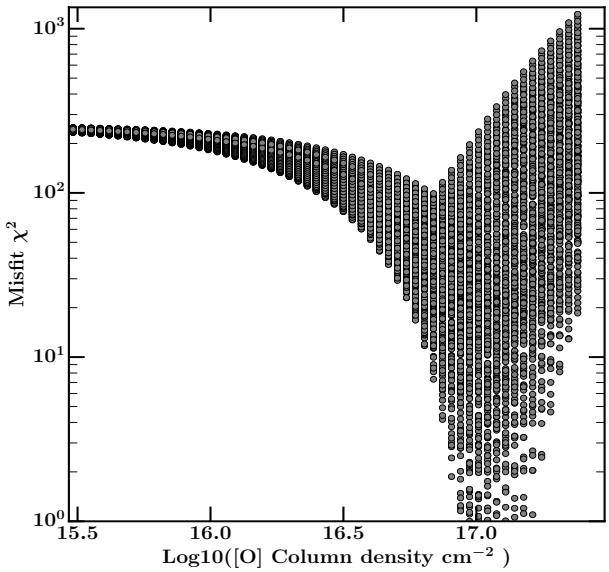

Fig. 2. Difference between measured and calculated radiance in terms of χ^2 vs. [O] column density. The gray circles stacking in vertical are for different ranges of surface temperature and Gauss convolution to simulate the LO broadening (see text for details).

The best-fit atomic oxygen column density estimate was accomplished through a brute-force grid search minimizing the χ^2 differences between measured and calculated radiances for a number of atmospheric scenarios. The atmospheric inputs were generated by scaling the beam-averaged atomic O VMR profile derived from v5.2 MCD, as discussed previously. In total, 60 scaling values were used, providing 30 points-per-decade in column density space, and then for each O VMR profile, an additional 14 variants were produced by varying the surface temperature between 200–265 K at 5 K steps. For each of the 840 synthetic radiance profiles a convolution with a Gaussian of varying width (3–21 MHz at 2 MHz step) was performed to simulate the additional LO broadening. The global view of the χ^2 fitting for all the different profiles described above is shown in Fig. 2. The best-fit profiles within the $\chi^2 \leq 3$ are shown in Fig. 3 as the gray envelope. The measured line with the 1σ noise error bars shows the measured spectrum, and the spectrum for the best fit is plotted in red.

Figures 2 and 3 illustrate that the mean column density is rather well constrained by the measured line and the column densities cluster in the confined space around the (mean) value 1.1×10^{17} cm^{-2} for the best-fitted spectra. Surprisingly, only a very narrow range of widths for the simulated Gaussian LO broadening is obtained (11, 13, and 12) MHz for the minimum, maximum, and average over the simulated spectra within the specified 3 χ^2 limit. This agrees well with a reasonable value of the LO jitter estimate. We took the spread of the retrieved column densities because the subsurface temperatures are varied to represent an estimate of uncertainty in the line contrast due to T_{atm}–T_{surf} uncertainties. We assumed that the line strength is known with an accuracy better than 3% (the JPL and HITRAN line strengths for this transition differ by about 1%), which leads to an additional uncertainty of ≈3% in the derived column density. The beam-averaged surface pressure is taken to be known within 5%, which results in 5% errors in the column density estimate. The root-sum-square uncertainty resulting from the atmospheric and spectroscopic input inaccuracies is estimated to be 18%.

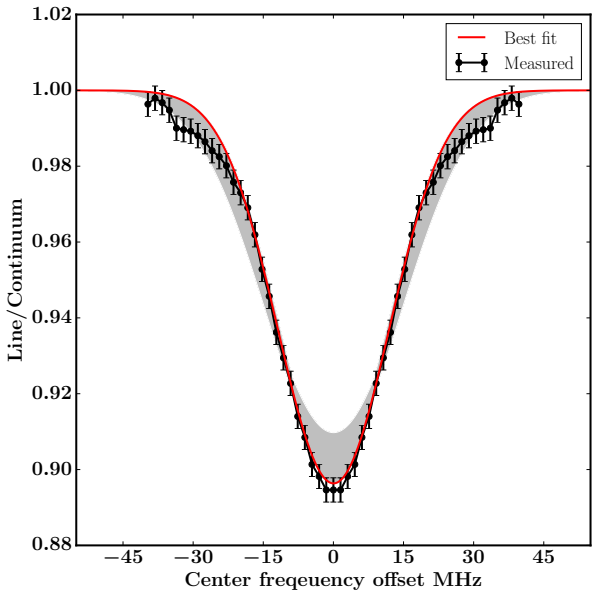

Fig. 3. Best-fit profile (red), all acceptable profiles within 3 χ^2 (gray), and the measured (symmetrized and centered) line (black; see text for discussion).

4. Summary and discussion

We have presented a measurement of the atomic oxygen fine-structure transition at 63 μm in the mesosphere of Mars by the GREAT instrument onboard the SOFIA observatory. This transition was observed for the first time in another terrestrial planet, allowing us to derive the [O] column density in the Martian upper atmosphere. The measured line profile is asymmetric with an extended blue wing that is assumed to be due to instrumental effects. In addition, the frequency scale calibration uncertainty did not allow us to reliably obtain a mean wind speeds at this time.

The line is detected in absorption against the Mars continuum, and our simulations indicate that it forms over a range of altitudes, 70–120 km. This observation was performed on May 14, 2014 corresponding to the Martian Ls = 130, with the beam center pointing at around 25 N. Despite an instrumental line broadening of the reference signal, we were able to constrain the Martian oxygen column density in a brute-force inversion. The best-fit column density, $(1.1 \pm 0.2) \times 10^{17}$ cm^{-2}, was found to be a factor of 2 below the predictions of the LMD model. Since the atomic oxygen is the main carrier of the chemical potential energy, it plays a prime role in the energy budget and chemistry of the upper atmosphere of Mars. The chemical modeling of the formation of ozone relies on the atomic oxygen and its transport across the nighttime terminator. In addition, the interpretation of the airglow measurements of electronically excited O_2 relies on the atomic O density because they efficiently quench the excited states. The atomic oxygen is known to have a significant long- and short-term variability (Hanson et al. 1977; Stewart et al. 1992; Valeille et al. 2010; Medvedev et al. 2015), and the respective modeling can be substantially improved based on measurements such as are now available from the SOFIA/GREAT instrument.

The detection of the OI line in the Martian atmosphere is an important accomplishment that will allow us to gain novel scientific knowledge on this atomic species, which is very difficult to obtain by any other method. The factor of 2 difference suggests that the LMD model, while not perfect, is a reasonably accurate representation of the mean oxygen in the upper Martian atmosphere, although a more robust validation is needed, requiring additional observations for different latitudes and local times. Future and long-term observations of this transition for different hemispheres and local solar times are highly desirable, and we will follow-up our results at the next Mars visibility, within scheduling constraints of the observatory, hopefully with a better control of the QCL.

Acknowledgements. Based on observations made with the NASA/DLR Stratospheric Observatory for Infrared Astronomy (SOFIA). SOFIA science mission operations are conducted jointly by the Universities Space Research Association, Inc, under NASA contract NAS2-97001, and the Deutsches SOFIA Institut, Universität Stuttgart under DLR Space Administration contract 50 OK 0901. SOFIA is carried out by the DLR Space Administration with funding by the Federal Ministry of Economics and Technology based on a resolution by the German Bundestag. The development of the QCL LO was supported under DLR Space Administration contract 50OK1104. We gratefully acknowledge the support by the observatory staff. Part of this work was supported by the German DFG project number HA3261/7-1. We thank E. Lellouch for his careful reading and helpful comments that improved the manuscript.

References

Barth, C. A., Stewart, A. I., & Hord, C. W. 1972, Icarus, 17, 457
Bertaux, J.-L., Korablev, O., Perrier, S., et al. 2006, J. Geophys. Res., 111, E10S90
Bougher, S. W., & Roble, R. G. 1991, J. Geophys. Res., 96, 11045
Büchel, D., Pütz, P., Jacobs, K., et al. 2015, IEEE Trans. Terahertz Sci. Technol., 5, 207
Chaufray, J. Y., Leblanc, F., Quémerais, E., & Bertaux, J. L. 2009, J. Geophys. Res., 114, 2006
de Graauw, T., Helmich, F. P., Phillips, T. G., et al. 2010, A&A, 518, L6
Forget, F., Hourdin, F., Fournier, R., et al. 1999, J. Geophys. Res., 104, 24155
Hanson, W. B., Sanatani, S., & Zuccaro, D. R. 1977, J. Geophys. Res., 82, 4351
Hartogh, P., Lellouch, E., Crovisier, J., et al. 2009, Planet. Space Sci., 57, 1596
Hartogh, P., Jarchow, C., Lellouch, E., et al. 2010a, A&A, 521, L49
Hartogh, P., Blecka, M. I., Jarchow, C., et al. 2010b, A&A, 521, L48
Heyminck, S., Graf, U. U., Güsten, R., et al. 2012, A&A, 542, L1
Huestis, D. L., Slanger, T. G., Sharpee, B. D., & Fox, J. L. 2010, Faraday Discuss., 147, 307
Jarchow, C., & Hartogh, P. 1995, in Global Process Monitoring and Remote Sensing of Ocean and Sea Ice, Proc. SPIE, 2586, 196
Klein, B., Hochgürtel, S., Krämer, I., et al. 2012, A&A, 542, L3
Krasnopolsky, V. A., & Feldman, P. D. 2002, Icarus, 160, 86
Krasnopolsky, V. A., & Krysko, A. A. 1976, Space Res., 16, 1005
Leblanc, F., & Johnson, R. E. 2002, J. Geophys. Res., 107, 5010
Mahaffy, P. R., Richard Hodges, R., Benna, M., et al. 2014, Space Sci. Rev., 185, 27
McClintock, W. E., Schneider, N. M., Holsclaw, G. M., et al. 2014, Space Sci. Rev., DOI: 10.1007/s11214-014-0098-7
McElroy, M. B., Kong, T. Y., Yung, Y. L., & Nier, A. O. 1976, Science, 194, 1295
Medvedev, A. S., González-Galindo, F., Yigit, E., et al. 2015, J. Geophys. Res., 120, 913
Mlynczak, M. G., Martin-Torres, F. J., Johnson, D. G., et al. 2004, J. Geophys. Res., 109, 12306
Nier, A. O., & McElroy, M. B. 1977, J. Geophys. Res., 82, 4341
Rengel, M., Hartogh, P., & Jarchow, C. 2008, Planet. Space Sci., 56, 1368
Richter, H., Greiner-Bär, M., Rösner, K., et al. 2015, IEEE Trans. Terahertz Sci. Technol., submitted
Rothman, L., Gordon, I., Babikov, Y., et al. 2013, J. Quant. Spectr. Rad. Transf., 130, 4, HITRAN2012 special issue
Sharma, R., Zygelman, B., von Esse, F., & Dalgano, A. 1994, Geophys. Res. Lett., 21, 1731
Stewart, A. I. F., Alexander, M. J., Meier, R. R., et al. 1992, J. Geophys. Res., 97, 91
Valeille, A., Bougher, S. W., Tenishev, V., Combi, M. R., & Nagy, A. F. 2010, Icarus, 206, 28
Zink, L. R., & Evenson, K. M. 1991, ApJ, 371, L85

Appendix A: Supporting material and figures

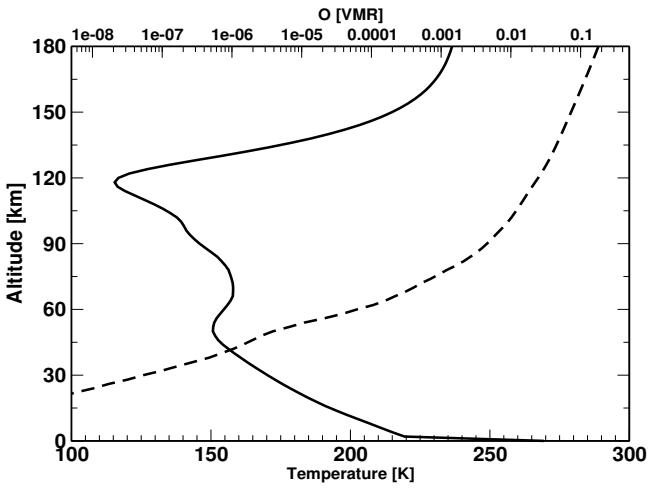

Fig. A.1. Vertical profile of temperature (solid line) and atomic oxygen VMR (dashed line) derived from the LMD v5.2 database that were used in the radiative transfer calculations.

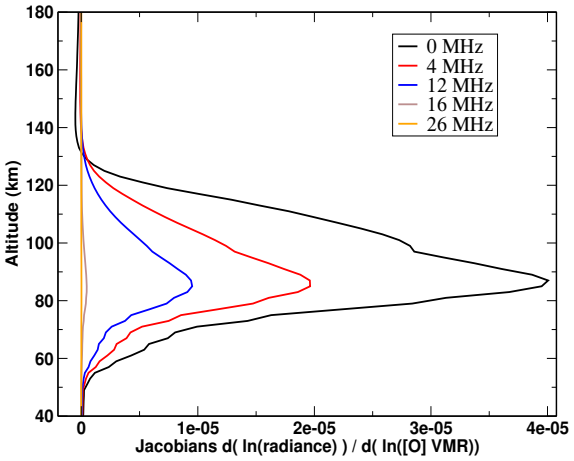

Fig. A.2. Calculated beam-averaged radiance sensitivity to changes in the O VMR (Jacobians) plotted for five frequency values shown as offsets. This calculation was performed for a column density of 8×10^{16} cm^{-2} , and the simulated LO smoothing with 10 MHz sigma was applied. For higher abundance (several times 10^{17} cm^{-2}), the line center peak shifts up to (100–110 km), with similar relative altitude shifts at other frequencies.

O contribution functions. The OI line is not completely optically thin ($\tau > 1$) for column densities higher than about 9×10^{16} cm^{-2}, and the observed line intensity forms at altitudes below 130 km, but over a rather extended altitude region, as shown in Fig. A.2. The sensitivity functions peak nearly at the same altitude for the different frequencies. This behavior is mainly due to the profile of the oxygen VMR profile, which extends from an insignificant value at 50 km to sharply increase with altitude, while the total density exponentially decreases, resulting in the [O] number density to have a peak just near the 90–100 km altitude and then smoothly decaying above. To a lesser degree, the "LO" broadening of the line, which was taken into account in these calculations, also plays a role in the degraded altitude resolution. In general, the wings of a Doppler line only depend on temperature and do not provide strong altitude information.